Journal of Magnetic Resonance 214 (2012) 144–150

Contents lists available at SciVerse ScienceDirect

Journal of Magnetic Resonance

journal homepage: www.elsevier.com/locate/jmr

# Spin evolution in a radio frequency field studied through muon spin resonance

Nigel J. Clayden [a,*], Stephen P. Cottrell [b], Iain McKenzie [b]

[a] School of Chemistry, University of East Anglia, Norwich NR4 7JT, United Kingdom
[b] Rutherford Appleton Laboratory, Harwell Science and Innovation Campus, Didcot OX11 0QX, United Kingdom

ARTICLE INFO

*Article history:*
Received 2 August 2011
Revised 19 October 2011
Available online 7 November 2011

*Keywords:*
Muon
Spectroscopy

ABSTRACT

The application of composite inversion pulses to a novel area of magnetic resonance, namely muon spin resonance, is demonstrated. Results confirm that efficient spin inversion can readily be achieved using this technique, despite the challenging experimental setup required for beamline measurements and the short lifetime (≈2.2 μs) associated with the positive muon probe. Intriguingly, because the muon spin polarisation is detected by positron emission, the muon magnetisation can be monitored during the radio-frequency (RF) pulse to provide a unique insight into the effect of the RF field on the spin polarisation. This technique is used to explore the application of RF inversion sequences under the non-ideal conditions typically encountered when setting up pulsed muon resonance experiments.



## 1. Introduction

Muon spin rotation involves implanting a positively charged muon ($\mu^+$) into a material, using a muon beam which is nearly 100% spin polarised and having an approximately circular spot of roughly 1 cm full width at half maximum at the sample position. After losing energy the muon comes to rest within 1 mm of the surface of the material, frequently thermalising at an interstitial location. At this site the muon is sensitive to the local electronic environment and the presence of local magnetic moments, both electronic and nuclear. Consequently the muon can be used as an extrinsic probe for the local chemical structure and magnetism [1]. In particular, because the muon behaves as a light isotope of hydrogen, the implanted muon can provide information on the local hydrogen environment which is complementary both to $^1$H NMR and neutron scattering [2].

Perhaps because of the short muon lifetime (~2.2 μs), muon spin rotation experiments are typically carried out without the use of external radio-frequency (RF) fields; the intrinsic polarisation of the spin-1/2 particle can be detected with great efficiency through the asymmetry in the positron emission which occurs as the muon decays. This is in marked contrast to NMR which depends on RF pulses for detection, and which, in turn, have permitted and encouraged a wide range of sophisticated experiments to be developed [3]. Indeed apart from one example of a spin echo [4] all the recent RF experiments have only used single RF pulses of varying duration either as simple 90° pulses of as longer nutation pulses. In principle many of the NMR experiments could be applied in muon spin resonance (μSR), with those associated with correlating the muon and nuclear spins being of particular interest since these would allow greater insight into the site of muon implantation. Currently though there is little experience at implementing more sophisticated RF pulse sequences at muon sources and thus it is difficult to assess the future value of even the most basic pulse sequences. This paper describes some preliminary steps towards implementing correlation methods through the use of composite pulses to demonstrate the feasibility of multi-pulse methods.

One practical reason why so few muon RF experiments have been performed [4] is the low instantaneous muon flux associated with the intense continuous muon beams such as TRIUMF [5] and PSI [6]. In order to compensate for the relatively small number of new polarised muons being implanted at any given instant, upon which the RF field can operate, a high duty cycle (typically 50%) is required that, in turn, results in excessive RF heating of both coil and sample. The full repertoire of RF techniques in μSR can therefore only sensibly be achieved at a pulsed muon source such as ISIS [7] and JPARC [8], where an appropriate timing can be set between the high intensity muon pulse (at ISIS, several hundred muons are typically implanted in a 70 ns wide pulse, with a pulse repetition frequency of 50 Hz) and the RF excitation [9]. The recent growth in the application of RF techniques in μSR has added a new dimension to the method, allowing, for example, the study of muon state kinetics [10], the determination of electron g-factors in muonium shallow donor states [11] and an investigation of muon-nuclear couplings [12].

A fundamental problem in all RF resonance experiments arises because the finite pulse lengths lead to pulse artefacts [13–19], and this is a particularly important consideration in quantum computing using NMR since these artefacts result in propagation errors [20]. In μSR [9,10,12] the potential for creating finite pulse arte-

* Corresponding author.
*E-mail address:* n.clayden@uea.ac.uk (N.J. Clayden).

1090-7807/$ - see front matter © 2011 Elsevier Inc. All rights reserved.
doi:10.1016/j.jmr.2011.10.018

facts is high for two reasons. Firstly, the large but poorly shaped coils (typically of dimension $20 \times 20 \times 2.5$ mm) that are used to maximise the sample area presented to the beam inevitably provide poor RF homogeneity over the sample volume, and secondly, the large coil volume results in a limited RF field strength, $B_1$, and therefore long RF pulses even when large RF powers are used. The large magnetogyric ratio of the muon (3.183 times that of the proton) only serves to accentuate the problem of having a limited RF field strength, as it leads to large dipolar interactions and thus off-resonance effects when X irradiation is required in μ-X spin systems. This is particularly true for $^1$H and $^{19}$F rich samples where, for example, in the case of $CaF_2$ the dipolar coupling between the muon and neighbouring fluorine nuclei is of the order of 220 kHz, and therefore typical pulses fail to excite the full frequency spectrum associated with the spin system and artefacts result. These are most clearly seen when a pulse having a specific function is applied. An example is the $\pi$ pulse that is used to invert the spin magnetisation [13,14] and refocus the chemical shift and magnetic inhomogeneity effects [15], where magnetisation which is off-resonance fails to invert properly or become refocussed.

One solution which has been applied in NMR [13–16], NQR [17], ESR [18] and MRI [19] is to use composite pulses, a sandwich of individual pulses of appropriate durations and phases that is designed to achieve a desired end with improved efficiency [16]. The composite pulse $\pi/2_x\ \pi_y\ \pi/2_x$ can be viewed as one of the simplest multiple pulse sequences, where two $\pi/2$ pulses are phase shifted by 90° from the central $\pi$ pulse to achieve spin inversion. Simulations show that the effect both of resonance offsets and RF inhomogeneities are much reduced by using such a pulse sequence [13], and this therefore provides a convenient test case for the implementation of multiple pulses in muon spin resonance, and in so doing will help facilitate the development of other multi-pulse experiments including combined muon and nuclear spin experiments.

Intriguingly, because the muon spin polarisation is detected by positron emission, the muon magnetisation can be monitored during the radio-frequency pulse, unlike in NMR, giving a unique insight into the effect of the RF on the spin polarisation. Moreover, a vector view of the polarisation can easily be obtained by applying appropriate detector groupings, experimental results can therefore be directly compared to simulation.

## 2. Experimental

The experiments were carried out using the MuSR spectrometer at the ISIS Pulsed Muon Facility, a full description of which can be found on the website [7] while the commissioning of a similar radio-frequency spectrometer at the facility is detailed in reference [9].

The time evolution of the muon spin polarisation is followed by means of 64 positron detectors arranged around the sample in order to measure the spatial distribution of the decay-positrons. Histograms are formed for each detector; data being typically collected for 32 μs following muon implantation at $t = 0$ μs, with the number of positrons detected during each 8 ns time-step being recorded. Each histogram can be described by an equation of the form:

$$N(t) = N_0 e^{-t/\tau_\mu}[1 + A(t)] \quad (1)$$

where $N_0$ is a normalisation factor related to the total counts and $\tau_\mu$ the muon lifetime. The information of interest, namely the frequency, amplitude, phase and depolarisation rate of the spin precession is contained in the muon asymmetry term $A(t)$. Appropriate grouping of the individual positron detectors enables a normalised decay asymmetry and hence muon polarisation to be revealed in three orthogonal directions. The typical longitudinal (or '$z$' axis) grouping is shown in Fig. 1a, where the 'red' and 'blue[1]' groups are defined forward (upstream) and backward relative to the initial muon spin polarisation. However, transverse groupings can also be defined to provide a measure of the polarisation along the '$x$' and '$y$' axes (shown in Fig. 1b and c respectively).

A normalised asymmetry, $A(t)$, with the muon lifetime removed, can be formed from the counts recorded in the two detector groups, $N_{RED}$ and $N_{BLUE}$, as follows

$$A(t) = \frac{N_{RED}(t) - \alpha N_{BLUE}(t)}{N_{RED}(t) + \alpha N_{BLUE}(t)} \quad (2)$$

where the factor $\alpha$ takes into account differences in detector efficiency within each group. The polarisation, $P(t)$, can then readily be obtained by comparing the measured signal asymmetry to an experimentally determined value for the maximum asymmetry, $A_0$, available for the particular detector grouping being considered:

$$P(t) = A(t)/A_0 \quad (3)$$

An RF asymmetry may also be defined to follow the time evolution of the muon spin polarisation under the influence of the RF field alone. This can be written in terms of the normalised asymmetries measured with and without the RF field as follows:

$$A^{RF}(t) = A^{RF_{ON}}(t) - A^{RF_{OFF}}(t) \quad (4)$$

Positive muons were implanted into a $CaCO_3$ test sample supplied by Johnson Matthey (purity 99.5%). This sample was chosen as muons thermalise predominantly into a diamagnetic state ($\mu^+$), which then evolves with minimal dipolar coupling as nuclear isotopes possessing spin are present only in low abundance. Field distributions and offsets could therefore be imposed on the sample and their effect investigated unambiguously. The fine powder material was contained in a Mylar packet (thickness 125 μm – transparent to the muon beam) and placed in the RF probe, with the coil tuned and matched to 50 Ω at 20 MHz to achieve $\mu^+$ resonance in a static field of 0.1476 T. The 90° phase shift required for the composite sequence was generated using a Mini-Circuits ZMSCQ-2-50 two way 90° power splitter, with the required RF phase being selected by switching the appropriate Mini-Circuits ZFSW-2-46 switch before recombining the signals to form an input to an AMT 3200 RF Amplifier. The phase balance between the two channels was checked using an oscilloscope, and cable lengths adjusted to achieve an optimal phase shift. RF powers of up to 300 W were employed (limited by RF breakdown), with the pulse lengths being determined by fitting the muon nutation frequency during a long RF pulse. An amplitude imbalance between the phase shifted channels required that the lengths of the $\pi/2_x$ and $\pi_y$ pulses had to be determined separately; in practice, muon nutation frequencies of ~252 kHz and a corresponding $\pi/2$ pulse length of ~1.0 μs were typical for our setup.

The RF probe was mounted in an Oxford Instrument helium exchange gas flow cryostat positioned in the muon beam, and all experiments were carried out at 295 K. Typically upwards of 200 million muon decay events were recorded for the composite pulse experiments in order that the signal could be clearly defined to at least seven muon lifetimes. A dual channel acquisition mode was used, with one channel containing a simple $\pi$ pulse while the other recorded data during a composite inversion sequence. As data taking in the two channels was interleaved, the performance of the composite and $\pi$ inversion pulses could be directly compared with the effect of equipment instabilities removed. To minimise the effect of resonance offsets on the experiment, the on-resonance con-

[1] For interpretation of colour in Figs. 1–5, the reader is referred to the web version of this article.

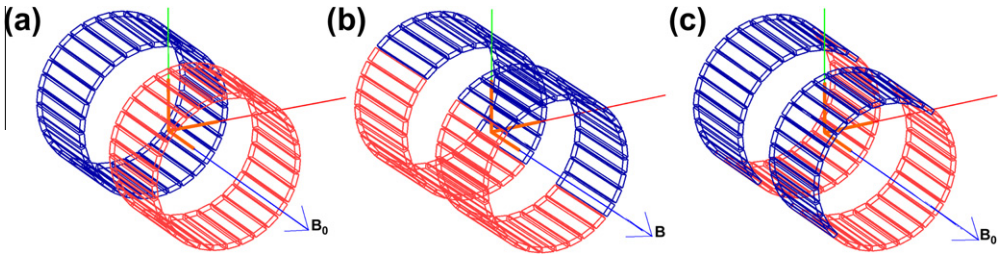


**Fig. 1.** Showing the instrument detector geometry and the detector groups (red and blue) used to obtain the signal asymmetry and hence muon polarisation in three orthogonal directions. The beam enters along the axis of the detector rings travelling into the page, and the sample is centred in the gap between the rings.

dition was itself established by a preliminary field scan using a defined muon RF frequency of 20 MHz and a step size of 0.5 mT.

## 3. Results and discussion

A simple demonstration of the poor RF field homogeneity provided by the coils used in the RF μSR experiment, and the effect this has on the signal, can be gained by following the muon response during a rotary echo refocusing sequence [21].

Rapid damping of the muon nutation is evident in Fig. 2a when a pulse of arbitrary duration is applied. In contrast, when the phase of the RF pulse is flipped by 180° after ~5.5 μs almost complete refocussing of the muon magnetisation is seen at ~11 μs (Fig. 2b). Therefore, we can be confident that RF field inhomogeneity is the origin of the damping of the muon signal in this experiment. A measure of this field inhomogeneity can be gained by using Eq. (4) to fit the signal decay measured in Fig. 2a. In practice two Gaussian components are required to adequately describe the muon response, $A^{RF_{ON}}(t)$ in the RF field, with one modelling the signal arising from muons stopped in the sample (within the RF coil) and another the signal arising from muons implanted in the coil former and the coil itself. A fit to the data is shown in Fig. 2a and gives a damping, $\sigma$, of the nutation signal from the sample of

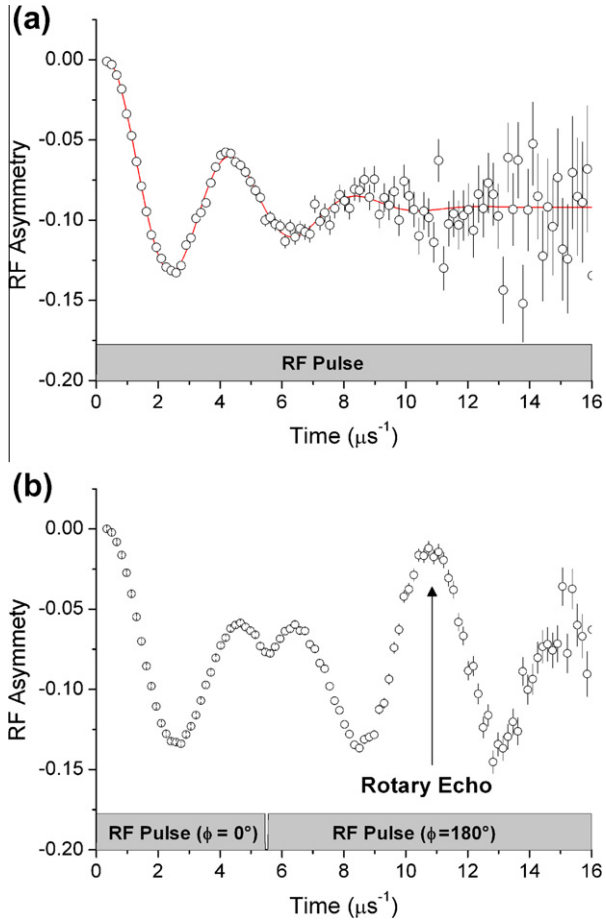


**Fig. 2.** (a) Evolution of the RF asymmetry for diamagnetic muons in a 0.1398 T static magnetic field during an RF pulse of arbitrary phase, and with an RF field of strength of 14.4 G. The decay is thought to be the result of inhomogeneity in the RF field. (b) The effect of switching the phase of the RF field by 180° after 4 μs. Essentially, complete refocussing is seen in a rotary echo formed at 8 μs, thereby demonstrating that the initial decay is the result of RF field inhomogeneity.

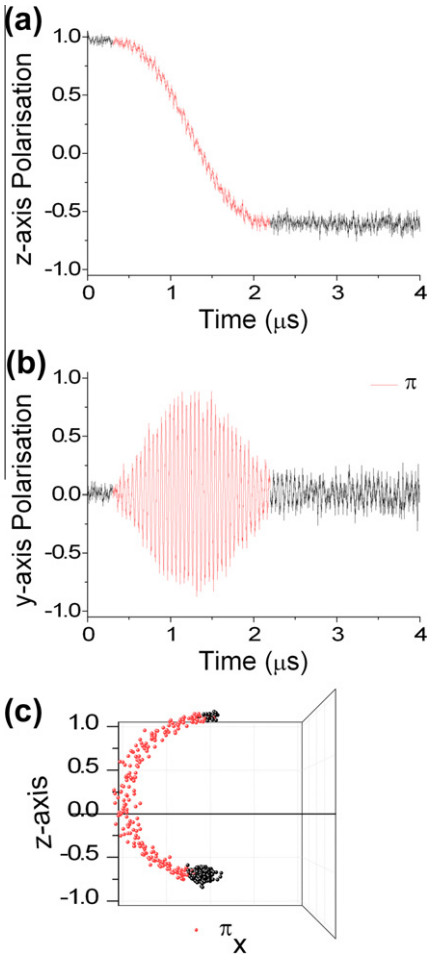


**Fig. 3.** Evolution of the (a) longitudinal (z-axis) and (b) transverse muon polarisation in a 0.1476 T static magnetic field whilst applying a simple 1.7 μs π pulse at resonance (20 MHz) with an RF field of strength 21.4 G. A fit to the transverse polarisation immediately following the RF pulse is shown. The trajectory of the polarisation during the simple inversion pulse is shown in (c), the results being displayed in a 20 MHz rotating reference frame with the view taken along the x'-axis.

0.174(17) $\mu s^{-1}$, suggesting a standard deviation for the RF field inhomogeneity of the order 174 kHz or 12.8 G. As expected, the second component comprises a smaller fraction of the measured signal (in a ratio of approximately 2:1), with the signal having a lower nutation frequency (~0.1 MHz) and a significantly enhanced damping (~0.3 $\mu s^{-1}$). Both are consistent with a signal arising from muons stopped in the highly inhomogeneous field outside and around the RF coil.

Longitudinal ($z$-axis) and transverse ($y$-axis) polarisation after a simple $\pi$ inversion pulse are shown in Fig. 3a and b respectively, while a plot of the trajectory of the polarisation vector is presented in Fig. 3c. Similar plots are shown in Fig. 4 for the $\pi/2_x\ \pi_y\ \pi/2_x$ composite inversion sequence. The effect on the signal of deliberately missetting pulse lengths is shown in Fig. 5, while the efficiency with which spin inversion is achieved as a function of resonance offset is described in Fig. 6.

Contrasting the change in $z$-axis polarisation for the simple $\pi$ inversion pulse (Fig. 3a) and composite sequence (Fig. 4a), starting from an initial polarisation close to one, the former achieves a final polarisation of −0.60(1) while the latter provides a significantly better polarisation inversion, with a final value of −0.76(1). To understand better the effect of RF field inhomogeneities on the operation of these pulse sequences, a final $z$-axis polarisation was estimated assuming the signal decay arising from the inhomogeneity is uncorrected by the sequence. Due regard was taken of the differing Gaussian decay rates arising from muons stopping within and around the RF coil, with the total signal weighted according to the muon fractions in each environment. Results are summarised in Table 1.

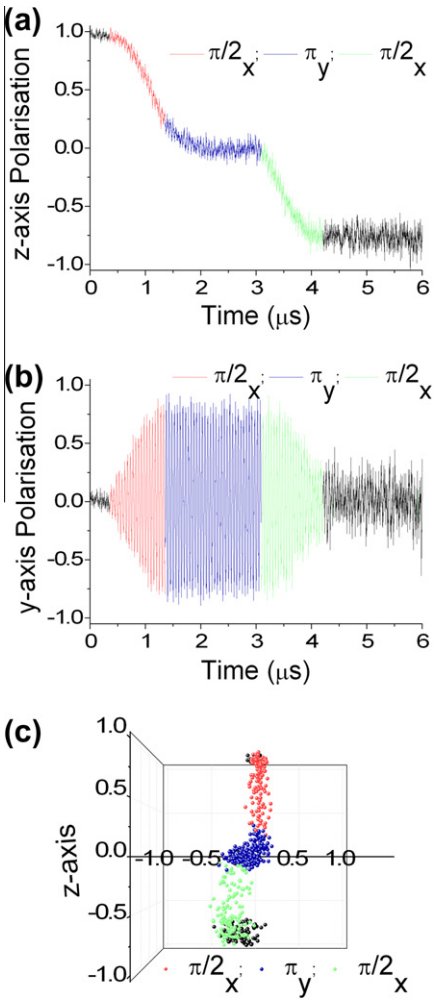


**Fig. 4.** Evolution of the (a) longitudinal (z-axis) and (b) transverse muon polarisation in a 0.1476 T static magnetic field whilst applying a composite inversion sequence ($\pi/2x\ \pi y\ \pi/2x$) at resonance (20 MHz) with an RF field of strength 18.6 G for the 1.0 μs $\pi/2x$ pulse and 21.4 G for the 1.7 μs $\pi y$ pulse. A fit to the transverse polarisation immediately following the RF pulse sequence is shown. The trajectory of the polarisation during the composite inversion sequence is shown in (c), the results being displayed in a 20 MHz rotating reference frame with the view taken along the y'-axis.

Clearly the simple $\pi$ pulse does not achieve the anticipated efficiency for polarisation inversion, and other factors must therefore be present and contribute to degrade its performance. In contrast, the final polarisation after the composite inversion sequence is larger than the calculated value, suggesting the sequence is, at least in-part, compensating for the RF field inhomogeneities and providing improved polarisation inversion. Considering this conclusion, it is puzzling that the transverse polarisation of 0.11(1) measured immediately following the composite inversion sequence (Fig. 4b) is comparable to the amplitude of the polarisation (0.09(1)) measured following the simple $\pi$ pulse (Fig. 3b). Unlike NMR, the action of each sequence can easily be investigated in more detail by modifying the analysis of existing data to display the time evolution of the polarisation during the RF excitation.

Considering first the simple $\pi$ pulse, fitting a cosine function to the $z$-axis polarisation shown in Fig. 3a yields a muon nutation frequency of 290(3) kHz, a value in excellent agreement with earlier calibration measurements utilising a long RF pulse and an ample demonstration of the stability of the experimental arrangement. While the behaviour of the corresponding transverse polarisation (Fig. 3b) is broadly as expected, the signal appears asymmetric about the signal maximum (corresponding to a rotation into the $x$–$y$ plane) that occurs at ~1.3 μs – with the pulse start set at ~0.3 μs and finish at ~2.2 μs, it appears that the RF pulse length is ~0.1 μs short. This is immediately confirmed by examining the polarisation trajectory during the $\pi$ pulse (Fig. 3c), which reveals the pulse length to be too short to provide the full $\pi$ rotation, and therefore a small component of the polarisation is left in the $x$–$y$ plane.

Three factors will contribute to the non-ideal behaviour of the pulses: resonance offsets, RF field inhomogeneity [13–15] and a combination of mis-set pulse lengths and pulse phase non-orthogonality. Indeed a detailed analysis of the $(\pi/2_x\ \pi_y\ \pi/2_x)$ composite inversion pulse in terms of the resonance offsets and RF field inhomogeneity has been presented [13]. Resonance offsets especially when combined with RF inhomogeneity could explain a large transverse component since the maximum relative offset of *ca* 0.1 gives a flip angle error of 10° or so and hence a transverse component of the order of 0.17 [13]. Yet if the relative resonance offset had been as large as this, one might have expected an even greater transverse component in the single pulse experiment as this is susceptible to the 2nd order RF field error while the composite pulse is susceptible to the 4th order field error [22]. However, this ignores the self-cancellation of the symmetric transverse components seen for a single 180° pulse if the RF inhomogeneity is symmetric. While for a composite pulse the resulting transverse components, though smaller, are asymmetric and so do not cancel. Thus is it entirely possible for the composite pulse to be performing better as an inversion pulse than the single pulse and yet still give larger transverse components. For the composite sequence, the response of the muon polarisation through the RF sequence can also be explained in terms of a mis-set initial $\pi/2_x$ pulse and then poor phase orthogonality between the RF channels. That the initial $\pi/2_x$ pulse is short is immediately confirmed by examining the $z$-axis polarisation (Fig. 4a), with a net positive polarisation remaining immediately following the RF pulse. As a result, the $\pi_y$ pulse rotates the polarisation about the $y$-axis as a small amplitude signal; the nutation frequency (and hence RF field strength) during this pulse is consistent with the calibrated value if due account is taken that the instantaneous gradient of this small amplitude ($A$) signal is given

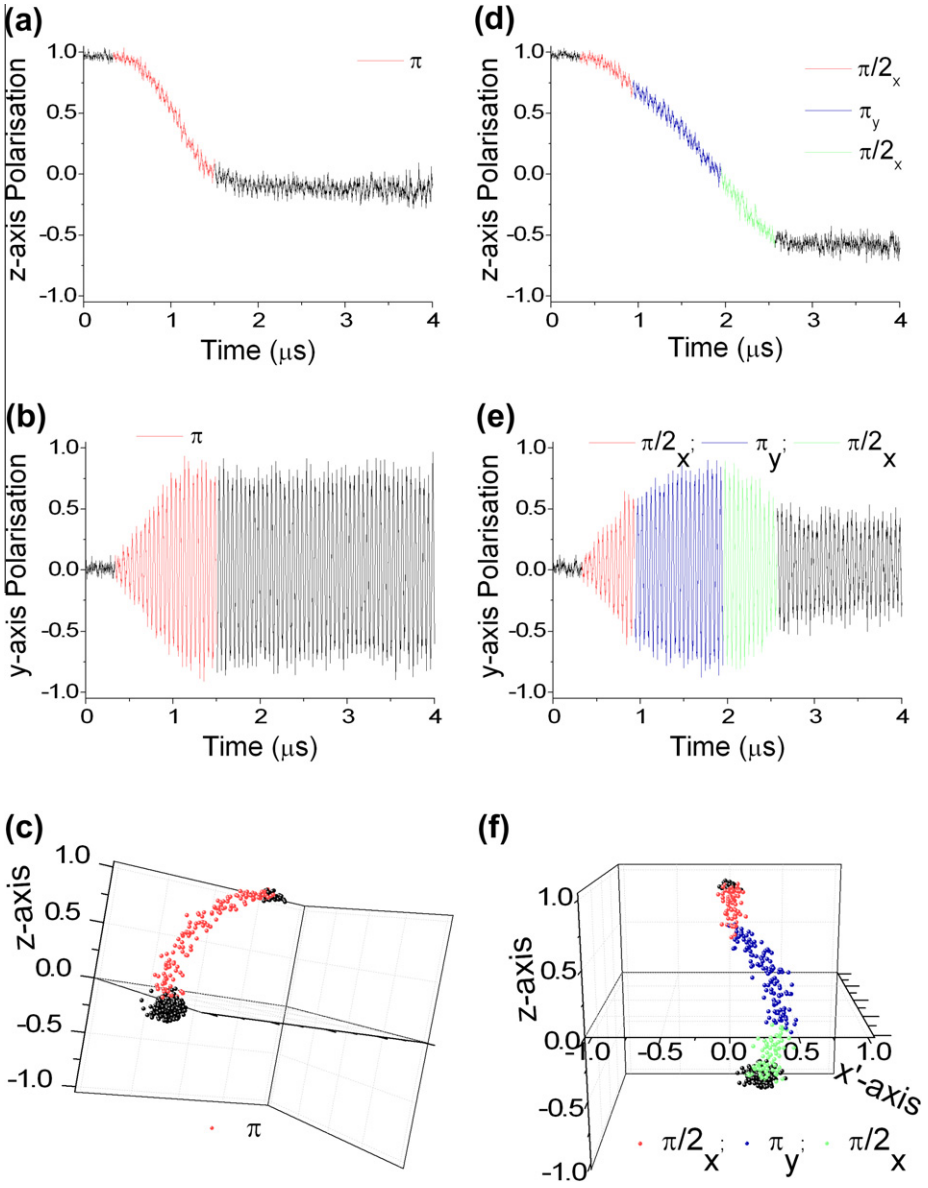


**Fig. 5.** Effect of misset RF pulses on simple π (a-c) and composite (d-f) RF sequences. Data measured in a 0.1476 T static magnetic field whilst applying RF pulses with a field of strength 18.6 G for the 0.6 μs π/2x pulse and 21.4 G for the 1.02 μs πy pulse – pulse lengths are reduced by ~40% compared with the optimum.

by the expression $-A\omega \cdot \sin(\omega t)$. This conclusion is consistent with the behaviour observed for the transverse polarisation (Fig. 4b); although the phase shifted $\pi$ pulse rotates the small $z$-axis component, it has no effect on the $y$-axis polarisation and a flat plateau is observed as expected. While the second $\pi/2_x$ pulse provides an efficient rotation of the polarisation to the -$z$-axis, the trajectory plot (shown in Fig. 4c) suggests that the inverted polarisation becomes offset in the $x$–$y$ plane, and it is this that gives rise to the small transverse polarisation that persists following the pulse sequence. It seems likely, however, that this offset is the result of incomplete phase orthogonality between the RF channels.

RF pulse length errors frequently occur in μSR experiments, both because of the variation in the RF field strength across the extended RF coil and the inherent difficulty in achieving well defined and calibrated microsecond-timescale RF pulses. The effectiveness of both simple ($\pi$ pulse) and composite ($\pi/2_x\ \pi_y\ \pi/2_x$) inversion sequences was therefore investigated with respect to quantified RF pulse errors. Experimental values for the $z$-axis polarisation immediately before and after application of the various pulse sequences were determined by fitting the polarisation curves and a normalised polarisation change deduced. The results are summarised in Table 2, and are in excellent agreement with predictions based on simulations using SIMPSON [23] to evaluate the final polarisation for the various experimental flip angles. Under optimum conditions both sequences achieved a similar measure of spin polarisation inversion, a value probably limited by the unique conditions required for the RF μSR experiment. However, as expected, the composite inversion sequence proved significantly more robust to mis-set pulse lengths than the simple $\pi$ inversion pulse, remaining effective even when gross (40%) errors were introduced. The latter case has been examined in more detail by studying the time evolution of the polarisation during both simple and composite inversion sequences, with results shown in Fig. 5.

Considering the RF power level, a spin rotation of ~118° is expected for the mis-set $\pi$ pulse, and this is reflected in the data by the transfer of a significant fraction of the polarisation from the $z$-axis (Fig. 5a) to the $y$-axis (Fig. 5b). A plot of the trajectory of the polarisation vector (Fig. 5c) confirms this, and also suggests that the spin rotation is smaller than expected, being closer to 90°. Similar plots are shown for the composite inversion sequence,

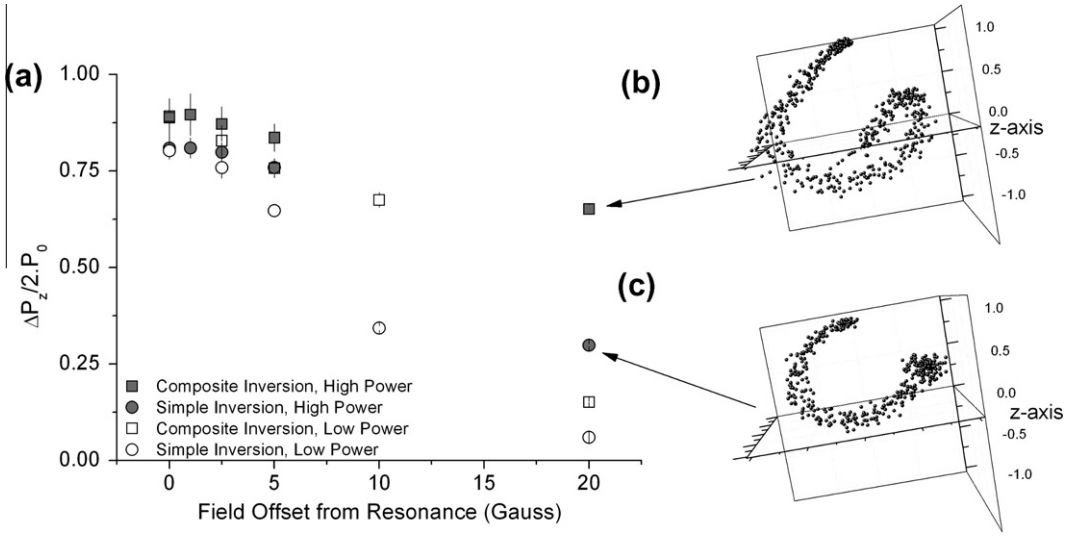


**Fig. 6.** Effect of RF power and the resonance offset on the effectiveness of the inversion of the muon polarisation, (a), using simple and composite sequences expressed as a change in normalised polarisation. Squares and circles correspond to the composite pulse and simple pulse respectively, with filled symbols representing an RF field strength, B1, of 21.4 G and unfilled symbols a field strength of 9.6 G. Trajectories of the polarisation during high power composite (b) and simple (c) inversion sequences carried out using a 21.4 G B1 field strength at a 20 G resonance offset are also shown.

**Table 1**
*z*-axis polarisation decay from RF field inhomogeneities and final signal estimated for inversion sequences. The values assume the signal decay arises from the RF inhomogeneity alone, and is uncorrected by the sequence. Final polarisations are calculated assuming a Gaussian signal decay, with values for the decay time constant and signal weighting as obtained by fitting the on-resonance decay shown in Fig. 2a.

| Inversion sequence | Total length (μs) | Pol. inside RF coil | W | Pol. outside RF coil | W | Total signal | |
|---|---|---|---|---|---|---|---|
| | | | | | | Calc | Exp |
| Simple $\pi$ | 1.7 | 0.91 | 2/3 | 0.77 | 1/3 | 0.87 | 0.60 |
| Composite | 3.7 | 0.66 | | 0.29 | | 0.54 | 0.76 |

**Table 2**
Experimental and simulated polarisation change for simple and composite inversion sequences. Optimum conditions are achieved using $\pi/2$ and $\pi$ pulses of 1 μs and 1.7 μs, respectively. Simulations were carried out using the SIMPSON [23] NMR simulation software package.

| Pulse length (μs) | | Actual flip angle (for '$\pi/2$' pulse) (°) | Simple inversion ($\pi$ pulse) ($\Delta P_z/2 \cdot P_0$) | | Composite inversion ($\pi/2_x\ \pi_y\ \pi/2_x$) ($\Delta P_z/2 \cdot P_0$) | |
|---|---|---|---|---|---|---|
| $\pi/2$ | $\pi$ | | Exp. | Sim. | Exp. | Sim. |
| 1 | 1.7 | 90 | 0.79(2) | – | 0.83(4) | – |
| 0.8 | 1.36 | 72 | 0.74(2) | 0.71 | 0.84(1) | 0.82 |
| 0.6 | 1.02 | 59 | 0.53(2) | 0.57 | 0.78(3) | 0.73 |

with Fig. 5d showing clear evidence for at least a partial inversion of the *z*-axis polarisation and Fig. 5e demonstrating that a component remains in the *x*–*y* plane. A detailed analysis of the polarisation trajectories (Fig. 5f), carried out by linear least squares fitting to the data measured during each pulse, suggests a phase error of ~18° between the initial $\pi/2_x$ and $\pi_y$ RF pulses. It is clear, therefore, that while our results demonstrate that the composite sequence offers a significantly more robust method of spin inversion for the μSR experiment, further gains may be possible by an improved experimental setup. The large samples typically used for μSR experiments can give rise to a static field distribution across the volume (this is of particular problem for the gas phase measurements currently under development), and therefore the effectiveness of the inversion sequences was explored as the static field was adjusted away from the resonance condition. The change in the *z*-axis polarisation was determined by fitting the polarisation curve before and after the RF sequence, and results from a series of measurements of varying offset fields and RF field strength, $B_1$, are shown in Fig. 6a. As expected, increasing resonance offsets lead to the inversion pulses becoming less effective, but with the composite pulse achieving a better inversion for all field offsets and RF field strengths measured. Importantly, for the small field offsets (<~2 G) typically encountered in solid state experiments, it is likely that the composite pulse will achieve uniform spin inversion across the full sample. The extreme field offsets measured (20 G) represent a shift from resonance approximately equal to that of the RF field strength (21.4 G), and therefore the effective field in the rotating reference frame makes an angle of ~45° with respect to the *z*-axis. Precession about the ~28 G resultant is clearly seen for the case of the simple $\pi$ inversion pulse (Fig. 6c), and while providing very poor spin inversion the possibility of transferring polarisation into the *x*–*y* plane under these unique conditions is amply demonstrated. The more complex polarisation trajectory arising from the composite sequence with its phase shifted RF pulses is shown in Fig. 6b; this clearly offers a more effective method of spin inversion.

## 4. Conclusions

The application of the composite inversion sequence to the RF μSR experiment has been demonstrated and shown to achieve

spin inversion with improved efficiency when compared to a simple $\pi$ pulse. The extended coil geometry used to maximise the sample area presented to the muon beam gives rise to both a highly inhomogeneous RF field and to resonance offsets, experiments confirm that each limits the efficiency with which simple pulse experiments can be executed. Recognising this, the composite inversion sequence was implemented as a proof-of-principle that more complex NMR sequences can be applied to μSR with the anticipated functional result. Measurements are encouraging, with a systematic study of the effect of pulse length errors and resonance offsets confirming the sequence to be robust to many of the artefacts that are common when using a simple $\pi$ pulse to invert the muon spin polarisation. Throughout this study, the unique potential for monitoring the muon magnetisation during the RF sequence has been exploited to provide a better understanding of how pulse errors develop; in itself, this may make μSR a useful technique for gaining a better understanding of spin evolution during RF sequences. The lifetime of the muon ($\sim$2.2 μs) contributes to the complexity of the experiment, requiring a timing accuracy and phase switching time that is beyond the capability of current NMR pulse programmers, and dictating the need for using high power RF into low Q coils to achieve short (sub-microsecond) and well defined RF excitations. Such technical developments are, however, quite feasible with current technologies, and therefore pulsed RF techniques appear to offer an interesting way of extending the scope of the μSR technique.

## Acknowledgments

The development of pulsed RF techniques for μSR has been supported by the European Commission under 6th Framework Programme through the Key Action: Strengthening the European Research Area, Research Infrastructures: Contract No.: RII3-CT-2003-505925, and the 7th Framework Programme through the Key Action: Strengthening the European Research Area, Research Infrastructures. Contact no: CP-CSA_INFRA-2008-1.1.1 Number 226507-NMI3. We thank the reviewers for helpful comments concerning the origin of the transverse components after the composite pulse.

## References

[1] in: S.L. Lee, S.H. Kilcoyne, R. Cywinski (Eds.), Muon Science, Muons in Physics, Chemistry and Materials, Proceedings of the Fifty First Scottish Universities Summer School in Physics, Institute of Physics Publishing, London, 1998.
[2] R. Kadono, K. Shimomura, K.H. Satoh, S. Takeshita, A. Koda, K. Nishiyama, E. Akiba, R.M. Ayabe, M. Kuba, C.M. Jensen, Phys. Rev. Lett. 100 (2008) 026401.
[3] R.R. Ernst, G. Bodenhausen, A. Wokaun, Principles of Nuclear Magnetic Resonance in One and Two Dimensions, Clarendon Press, Oxford, 1987.
[4] S.R. Kreitzman, Hyperfine Interactions 65 (1990) 1055.
[5] TRIUMF, Canada's National Laboratory for Particle and Nuclear Physics, http://www.triumf.info/.
[6] Laboratory for Muon Spin Spectroscopy, Paul Scherrer Institute, http://lmu.web.psi.ch/.
[7] The ISIS Pulse Muon Facility, http://www.isis.stfc.ac.uk/groups/muons/.
[8] Japan Proton Accelerator Research Complex, http://j-parc.jp/index-e.html.
[9] S.P. Cottrell, S.F.J. Cox, C.A. Scott, J.S. Lord, Physica B 289–290 (2000) 693.
[10] Y. Morozumi, K. Nishiyama, K. Nagamine, Phys. Rev. Lett. A 118 (1986) 93.
[11] J.S. Lord, S.F.J. Cox, H.V. Alberto, J.P. Duarte, R.C. Vilao, J. Physics-Condensed Matter 16 (2004) S4707.
[12] .N.J. Clayden, S.P. Cottrell, Phys. Chem. Chem. Phys. 8 (2006) 3094.
[13] M.H. Levitt, R. Freeman, J. Magn. Reson. 33 (1979) 473.
[14] R. Tycko, H.M. Cho, E. Schneider, A. Pines, J. Magn. Reson. 61 (1985) 90.
[15] M.H. Levitt, R. Freeman, J. Magn. Reson. 43 (1981) 65.
[16] M.H. Levitt, Composite pulses, Prog. NMR Spectroscopy 18 (1986) 61.
[17] V.T. Mikhaltsevitch, T.N. Rudakov, J.H. Flexman, P.A. Hayes, W.P. Chisholm, Solid State Nucl. Magn. Reson. 25 (2004) 61.
[18] J.J.L. Morton, A.M. Tyryshkin, A. Ardavan, K. Porfyrakis, S. A Lyon, G. Briggs, D. Andrew, Phys. Rev. Lett. 95 (2005) 200501/1.
[19] C.M. Collins, Z. Wang, W. Mao, J. Fang, W. Liu, M.B. Smith, Mag. Reson. Medicine 57 (2007) 470.
[20] W.G. Alway, J.A. Jones, J. Magn. Reson. 189 (2007) 114.
[21] I. Solomon, Phys. Rev. Lett. 2 (1959) 301.
[22] M. H. Levitt, Composite Pulses, in: D.M. Grant, R.K. Harris (Eds.), Encyclopedia of Nuclear Magnetic Resonance, Wiley, 1996.
[23] M. Bak, J.T. Rasmussen, N.C. Nielsen, J. Magn. Reson. 147 (2000) 296.